Astron. Astrophys. 122, 73–78 (1983)

ASTRONOMY AND ASTROPHYSICS

Accretion onto rotating, magnetic neutron stars: the inner edge of the disk

U. Anzer and G. Börner

Max-Planck-Institut für Physik und Astrophysik, Institut für Astrophysik, Karl-Schwarzschild-Strasse 1, D-8046 Garching bei München, Federal Republic of Germany

Received June 30, 1982; accepted January 3, 1983

Summary. The surface of an accretion disk in a rotating neutron star's magnetic field is subject to the Kelvin-Helmholtz instability induced by the velocity difference of the rigidly rotating magnetosphere and the Keplerian disk. This instability is analysed in a simplified geometry. It is shown that a large part of the disk surface will become unstable, leading to a turbulent diffusion of the disk plasma into the magnetosphere. The resulting exchange of angular momentum between the neutron star and the accreting matter is described. The present model of a magnetic dipole axis perpendicular to the rotation axis of the neutron star is compared to the model of an aligned rotator. The observational consequences with respect to the rotational state of pulsating X-ray sources are discussed.

Key words: accretion disks – magnetic neutron stars – pulsating X-ray sources

I. Introduction

In a previous paper (Anzer and Börner, 1980) we have shown that the surface of an accretion disk in a rotating neutron star's magnetic field is subject to the Kelvin-Helmholtz instability induced by the velocity difference of the corotating magnetic field ($v_\phi = \Omega r$) and the Keplerian disk ($v_\phi = (GM/r)^{1/2}$). A simple configuration was adopted, where the dipole axis of the stellar magnetic field was in the plane of the disk, perpendicular to the star's rotation axis. The configuration ist not as special, as might seem at first glance, because calculations of the field of an oblique magnetic dipole – inclined by less than 90° to the rotation axis in – the presence of an idealized accretion disk (infinitely thin and infinitely conducting) (Riffert, 1980; Aly, 1980; Kundt and Robnik, 1980) showed that the distribution and the shape of the field lines around the inner edge of the disk is quite similar for a wide range of angles of inclination: in these cases there were two neutral points on the surface of the disk which separate two regimes of field lines. One finds that for inclination angles larger than 70° these points lie at $r \lesssim 1.03\, r_m$, and at r_m for the perpendicular configuration. Thus, the perpendicular configuration can be considered a good approximation for many cases.

Our previous analysis (Anzer and Börner, 1980) has been restricted to a purely hydrodynamic treatment of the instability, assuming equal sound speeds on both sides of the boundary. In the present paper we extend these previous calculations to incorporate the magnetic field, and to allow for different sound speeds in the disk and in the magnetosphere. The actual analysis is still restricted to a simplified geometry: a plane boundary separating the 2 media, with constant densities and constant magnetic fields on each side.

We also give a qualitative discussion of the interaction region in a more realistic configuration. We discuss to some extent the model of an aligned rotator advocated by Ghosh and Lamb (1979). Finally the observational consequences of the 2 different models are discussed.

Send offprint requests to: U. Anzer

II. Analysis of the Kelvin-Helmholtz instability

We investigate the stability of the plane interface between 2 media. Medium 1 is moving with velocity $\Delta \boldsymbol{v}$ parallel to the boundary. Small disturbances of the form

$$\boldsymbol{\xi} = \boldsymbol{\xi}_0 e^{i(\boldsymbol{k}\boldsymbol{x} - \omega t)}$$

are then analysed.

Take the velocity $\Delta \boldsymbol{v}$ to form an angle α with the component of the wave vector $\boldsymbol{k}_t = (k_x, k_y, 0)$ which is along the interface (see Fig. 1), and angles β_1, β_2 with the magnetic fields $\boldsymbol{B}_1, \boldsymbol{B}_2$ in medium 1 or 2. The z axis is normal to the boundary $z=0$. The dispersion equation is then given by (Frejer, 1964):

$$\frac{\varrho_1^2[V_1^2\cos^2(\alpha-\beta_1)-w^2]^2}{1-\dfrac{\varrho_1^2[V_1^2\cos^2(\alpha-\beta_1)-w^2]^2}{w^4}} = \frac{\varrho_2^2[V_2^2\cos^2(\alpha-\beta_2)-(w-\Delta v\cos\alpha)^2]^2}{1-\dfrac{(w-\Delta v\cos\alpha)^4}{(w-\Delta v\cos\alpha)^2(u_2^2+V_2^2)-u_2^2V_2^2\cos^2(\alpha-\beta_2)}}, \tag{2.1}$$

where $w = \omega/k_t$; ϱ_i: density, u_i: sound velocity, V_i: Alfvén velocity in medium i.

Let us look at the special case $u_2 = 0$, $V_1 = 0$, i.e. no magnetic field in medium 1, dominating Alfvén velocity in medium 2.

Set

$$V_2 \equiv V_A, \quad u_1 \equiv c_s, \quad x \equiv \frac{\Delta v\cos\alpha}{V_A}, \quad m \equiv \frac{w}{c_s}.$$

When then obtain from (2.1)

$$\varrho_1^2 w^4\left(1-\left[m\frac{c_s}{V_A}-x\right]^2\right) = \varrho_2^2 V_A^4\left(\cos^2(\alpha-\beta)-\left[\frac{mc_s}{V_A}-x\right]^2\right)^2(1-m^2). \tag{2.2}$$

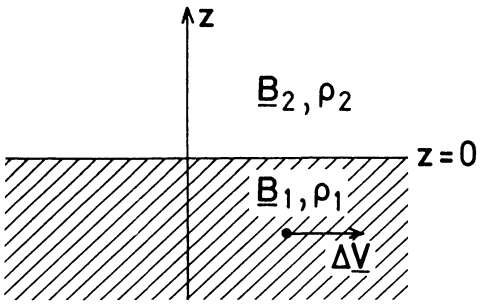

Fig. 1. A plane boundary configuration

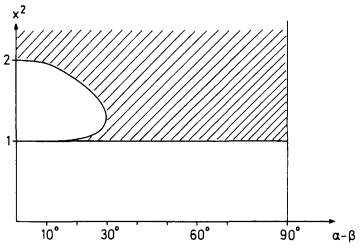

Fig. 2. $x^2=(\Delta v/V_A\cos\alpha)^2$ is plotted against $(\alpha-\beta)$. The shaded region is stable

Pressure equilibrium gives $\varrho_1 c_s^2=\frac{1}{2}\varrho_2 V_A^2$, and we can therefore write

$$\frac{m^4}{4}\left[1-\left(m\frac{c_s}{V_A}-x\right)^2\right]=\left[\cos^2(\alpha-\beta)-\left(\frac{mc_s}{V_A}-x\right)^2\right]^2(1-m^2). \quad (2.3)$$

A sufficient condition for stability is satisfied if all the roots m of Eq. (2.3) are real. We shall assume $c_s/V_A\equiv 1/a\ll 1$ throughout the analysis. To find (approximately) the roots of (2.3) we define $y\equiv(m/a)-x$, and rewrite (2.3) as

$$(1-y^2)(x+y)^4=4(\cos^2(\alpha-\beta)-y^2)^2\left(\frac{1}{a^4}-\frac{1}{a^2}(x+y)^2\right). \quad (2.4)$$

Looking at (2.4) as a polynomial in a, we can determine the solutions as power series in $1/a$ to arbitrary accuracy. We consider various regimes:

A. For y of order 1, we see from the leading term that $y\simeq 1$ is one root, i.e. $m_1=a(1+x)$. m_1 is real, and also the next term of the expansion is real:

$$y\simeq 1+\frac{2}{a^2}\frac{(\cos^2(\alpha-\beta)-1)^2}{(1+x)^2}. \quad (2.5)$$

B. Next we take $m/a=(y+x)\equiv\varepsilon\ll 1$, then dividing (2.4) by $(1-y)$, we arrive at

$$\varepsilon^4(1-x+\varepsilon)=\frac{4(\cos^2(\alpha-\beta)-(\varepsilon-x)^2)^2}{(1+x-\varepsilon)}\left(\frac{1}{a^4}-\frac{\varepsilon^2}{a^2}\right). \quad (2.6)$$

B 1. For $x\neq 1$, i.e. $|1-x|\gg\varepsilon$, we have

$$\varepsilon^4(1-x)=\frac{4(\cos^2(\alpha-\beta)-x^2)}{(1+x)}\left(\frac{1}{a^4}-\frac{\varepsilon^2}{a^2}\right)$$

and this yields immediately

$$m^2\equiv a^2\varepsilon^2=\frac{2}{(x^2-1)}\{(\cos^2(\alpha-\beta)-x^2)^2\pm[(\cos^2(\alpha-\beta)-x^2)^4 -(x^2-1)(\cos^2(\alpha-\beta)-x^2)^2]^{1/2}\} \quad (2.7)$$

(2.7) gives us 4 roots m_2, m_3, m_4, m_5.

For stability we must have $m^2>0$, which requires

$$x^2>1, \quad (2.8)$$

and in addition the expression under the square root in (2.7) must be positive: Hence

$$[x^2-\cos^2(\alpha-\beta)]^2>(x^2-1) \quad (2.9)$$

which is equivalent to (2.10) (for $\cos^2(\alpha-\beta)>\frac{3}{4}$; if $\cos^2(\alpha-\beta)<\frac{3}{4}$ (2.9) does not lead to an additional condition)

$$x^2>\cos^2(\alpha-\beta)+\tfrac{1}{2}+(-\tfrac{3}{4}+\cos^2(\alpha-\beta))^{1/2}. \quad (2.10)$$

In Fig. 2 we have shaded the regions of stability. Two have stability for all possible values of α and β, requires

$$x^2\geqq(\tfrac{3}{2}+\sqrt{\tfrac{1}{4}})=2.$$

For $x\neq 1$, the last root is

$$m_6=-a(1-x). \quad (2.11)$$

Similar to (2.5) corrections to the roots given in (2.7) and (2.11) can be determined.

B 2. For $x=1$, the Eq. (2.6) contains an ε^5-term:

$$\varepsilon^5=2(\cos^2(\alpha-\beta)-1)^2\left(\frac{1}{a^4}-\frac{\varepsilon^2}{a^2}\right). \quad (2.12)$$

In lowest order

$$\varepsilon_{2,3}=\pm\frac{1}{a}, \quad (2.13)$$

$$\varepsilon_{4,5,6}=(-2(\cos^2(\alpha-\beta)-1)^2)^{1/3}a^{-2/3}e^{i(2\pi/3)n}, \quad n=0,1,2. \quad (2.14)$$

The next higher order corrections can be easily computed, and then

$$\varepsilon_{2,3}=\frac{1}{a}\left\{\pm 1-\frac{1}{4(\cos^2(\alpha-\beta)-1)^2}\frac{1}{a}\right\}, \quad (2.15)$$

or $m_{2,3}=a\varepsilon_{2,3}$

$$\varepsilon_{4,5,6}=-(2(\cos^2(\alpha-\beta)-1)^2)^{1/3}a^{-2/3}e^{i(2\pi/3)n} -\tfrac{1}{3}(2(\cos^2(\alpha-\beta)-1)^2)^{1/3}((1-\cos^2(\alpha-\beta) \cdot(7+\cos^2(\alpha-\beta))-1))a^{(-4/3)}e^{-i(2\pi/3)n} \quad (2.16)$$

For $x^2\leqq 1$ there are modes with complex values of m. But not all of these are physically acceptable unstable modes concentrated around $z=0$, i.e. decreasing exponentially for growing $|z|$. This is satisfied, if $\mathrm{Im}(k_{z1})<0$ (in medium 1) and $\mathrm{Im}(k_{z2})>0$ (in medium 2). According to Fejer (1964) we have

$$\left(\frac{k_{z1}}{k_t}\right)^2=-1+m^2, \quad (2.17)$$

$$\left(\frac{k_{z2}}{k_t}\right)^2=-1+\left(\frac{m}{a}-x\right)^2, \quad (2.18)$$

and the continuity of the disturbances at the boundary $z=0$ requires

$$-\frac{m^2}{k_{z1}}=2\frac{\cos^2(\alpha-\beta)-(m/a-x)^2}{k_{z2}}. \quad (2.19)$$

Since $m/a\ll 1$, these conditions on $\mathrm{Im}(k_z)$ and Eqs. (2.17)–(2.19) lead to

$$x^2-\cos^2(\alpha-\beta)\geqq 0 \quad (2.20)$$

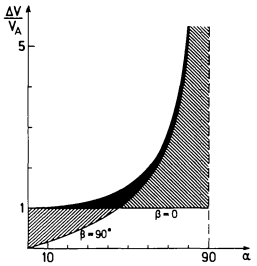

Fig. 3. Angles α for which instability occurs. The shaded regions are unstable. 2 cases $\beta=90°$ and $\beta=0°$ are shown

for unstable modes. On the other hand, $x^2 \leqq 1$, i.e.

$$\frac{1}{\cos^2\alpha} \geqq \frac{\Delta v}{V_A} \geqq \frac{\cos^2(\alpha-\beta)}{\cos^2\alpha}. \tag{2.21}$$

We have shown the permitted range of angles α in Fig. 3 for 2 values of β($\beta=0$, i.e. magnetic field parallel to the flow velocity, and $\beta=\frac{\pi}{2}(\Delta \boldsymbol{v} \perp B)$).

For $\beta=0$,

$$\frac{1}{\cos\alpha} \geqq \frac{\Delta v}{V_A} \geqq 1;$$

for $\beta=\dfrac{\pi}{2}$

$$\frac{1}{\cos\alpha} \geqq \frac{\Delta v}{V_A} \geqq \tan\alpha.$$

For increasing $\Delta v/V_A$, the range of angles α becomes increasingly smaller.

For $x^2>2$ all the 6 roots of Eq. (2.3) are real. The condition for stability $x^2>2$ can be rewritten using the condition of pressure equilibrium $\varrho_1 c_s^2=\frac{1}{2}\varrho_2 V_A^2$, as

$$\Delta v \cos\alpha > \sqrt{2} V_A = 2\left(\frac{\varrho_1}{\varrho_2}\right)^{1/2} c_s. \tag{2.22}$$

In an earlier paper we had found the stability condition $\Delta v \cos\alpha \geqq 2\sqrt{2} c_s$. In general $\varrho_2 \ll \varrho_1$, and therefore the region of instability is far more extended than in the simplified model of Paper I. For example, if $\varrho_1=100\,\varrho_2$, then

$\Delta v \cos\alpha \geqq 20\, c_s$

for stability.

Translating this result into the disk geometry, we may conclude that inside a ring around r_c, where $|\Delta v| \leqq 20\, c_s$, all k-modes can grow exponentially. Outside of this ring, one soon has $|\Delta v| \gg 20\, c_s$, therefore only k-modes with $|\cos\alpha| \ll 1$ (i.e. with $\boldsymbol{k}$ almost perpendicular to $\Delta \boldsymbol{v}$ can grow). There are, however, always some $\boldsymbol{k}$-modes which can grow – to first order in $1/a$ these modes have imaginary m, i.e. phase velocity zero. Thus the whole surface of the disk can become unstable.

Now in most parts of the unstable disk the kinetic energy density of the matter $\frac{1}{2}\varrho_1(\Delta v)^2$ exceeds the energy density in the magnetic field:

$$\frac{1}{2}\varrho_1(\Delta v)^2 \simeq \frac{1}{2}\varrho_1(20\, c_s)^2 \gg \frac{1}{2}\varrho_1 c_s^2 = \frac{1}{2}\frac{B^2}{8\pi}. \tag{2.23}$$

Therefore the disk material which diffuses into the magnetosphere because of the instability will lead to a strong winding-up of the field, and a large azimuthal component B_ϕ will then develop. Since pressure equilibrium with the dipole field outside the interaction region has to be maintained, B_ϕ will be limited by the dipole value of B. If the field is wound up to greater strength, it will just expand in the vertical direction. One can imagine that the final result will be the formation of a layer above the unperturbed disk surface. A detailed investigation of this layer will be done in a future paper. Here we shall only give a descriptive presentation. In the z-direction away from the disk there will first be a region, where

$$\frac{1}{2}\varrho(\Delta v)^2 \gg \frac{B^2}{8\pi}$$

holds. Here the magnetic field has to follow the fluid motion and therefore $\boldsymbol{B}=B_\phi \boldsymbol{e}_\phi$, also $v_\phi=v_k$. But because of the increase in magnetic pressure and the action of gravity the density will decrease in the outward z-direction. Then a height is reached where the density becomes sufficiently low that the angular momentum of the disk material can be taken up by the magnetic field. From there on the field can relax to the dipole configuration i.e. B_r will increase from zero to the dipole value. Inside the corotation radius this interaction leads to a slowing down of the gas, $v_\phi<v_k$, which results in a radial net inward force. Therefore the accretion can occur out of this layer. For $r>r_c$ a similar outward flow will be driven by the magnetic field.

III. Discussion of the aligned rotator model

The alignment of rotation and dipole axis of the neutron star leads to an axisymmetric configuration. This looks simpler at a first glance, and has therefore received considerable attention (Ghosh and Lamb, 1979a, b; Ghosh et al., 1977). The details of the interaction between disk matter and stellar fields are, however, as intricate problems as in the less symmetric case discussed in Sect. 2. One basic difficulty is, of course, that accretion onto the magnetic poles of the neutron star does not lead to pulsed emission in the axisymmetric case.

In this case the diamagnetic properties of the plasma would prohibit the penetration of field lines through the disk, and the field lines near the magnetic equator would bend in and follow the disk surface tangentially. It has been argued (Ghosh and Lamb, 1979a) however, that such a magnetosphere with strong, oppositely directed magnetic fields above and below the disk could not be maintained. Instead, rapid reconnection of field lines through the disk is advocated, introduced in the model by an effective electrical resistivity. The ratio of the reconnection speed to the Alfvén velocity is adopted as 0.1–1. It is then assumed that a balance between shear amplification and reconnection of magnetic field lines can be maintained, leading to ratios of azimuthal field B_ϕ and vertical field B_z of $B_\phi/B_z=1$–10. The assumed effective resistivity gives rise to a boundary layer structure. Mass flow onto the field lines takes place in this thin boundary layer.

Across the boundary layer, as one goes into the disk, the magnetic field strength decreases by an order of magnitude, the azimuthal motion changes from nearly corotational to nearly Keplerian. The accreting matter, and the magnetic torque inside the corotation radius $r_c(r_c=(GM/\Omega^2)^{1/3})$ accelerate the stellar rotation, while the torque from the disk beyond r_c leads to braking.

Various aspects of the model have remained open to doubt and criticism:

1. The aligned rotator model cannot explain the X-ray pulsations. A regular time variation in the radiation pattern must be due to an inclination of the dipole axis to the rotation axis.

2. The reconnection speed is given a rather high value. Ghosh and Lamb (1979a, b) use an estimate based on X-type magnetic field configurations. The physical situation in the disk geometry may, however, reduce this mechanism.

In X-type reconnection processes the field is dissipated rapidly when the magnetic field energy can be taken up as kinetic energy of plasma motion. In a Keplerian disk, however, the motion of the material is restrained.

3. In their paper Ghosh and Lamb want to make use of the concept of small scale magnetic fields in the disk which connect to the large scale stellar field. Then convection driven by a temperature gradient should transport the magnetic fields through the disk. It is by no means clear, however, that such a convective pattern will produce the desired rapid field connection across the disk.

4. Finally, their estimates give a magnetic field in the disk which is considerably weaker (by a factor $\frac{1}{5}$) than the undisturbed dipole field. Therefore about $\frac{4}{5}$ of the magnetic flux which would pass through the disk in the unperturbed dipole case, now has to be squeezed through the hole in the disk ($r \leqq r_M$). In Fig. 4 we have tried to illustrate this situation by superimposing $\frac{4}{5}$ of the field of a dipole + disk solution (Aly, 1980; Riffert, 1980; Kundt and Robnik, 1980), where the disk is taken to be ideally conducting, and $\frac{1}{5}$ of an unperturbed dipole solution. The resulting field deviates significantly from a dipole, and it generates a severe problem for the accretion flow: the field lines threading the boundary layer all extend to large radial distances before they approach the magnetic poles. Therefore a mass flow along $\boldsymbol{B}$ would at first have to flow outwards in the gravitational potential, which seems impossible.

Thus, even if we accept the general features of the construction by Ghosh and Lamb (1979), we should remark that an essential problem of the accretion flow has not been solved in their model. Probably additional Kelvin-Helmholtz or Rayleigh-Taylor instabilities of the matter in the magnetic field have to be considered in the aligned rotator model. It seems to us that in this case even the question whether accretion occurs at the magnetic poles or at the equator cannot be easily decided.

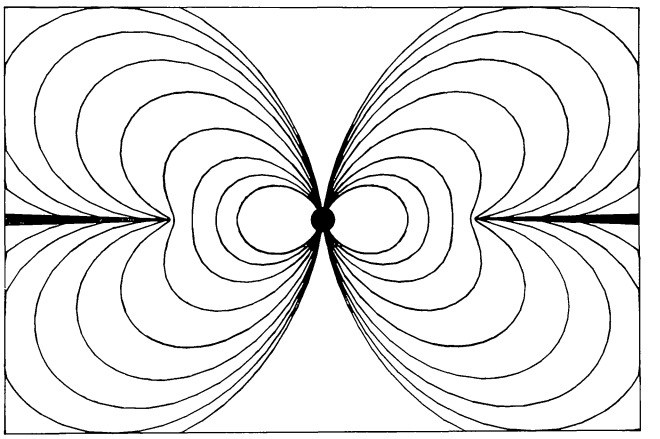

Fig. 4. Aligned rotator with $\frac{1}{5}$ of the flux through the disk (Neutron star not drawn to scale)

IV. Theory and observations

The theoretical considerations presented above of the interaction between disk matter and the neutron star's magnetic field have some immediate consequences: Matter which gets onto the magnetic field lines exchanges angular momentum with the neutron star. A detailed quantitative model – which does not exist yet – would determine the amount δJ of angular momentum transferred to the star. Now, if the neutron star reacted as a rigid body, its own angular momentum would change corresponding to

$$I\left(\frac{2\pi}{P}\right)\dot{P}/P = \delta J\,, \tag{4.1}$$

where I is the moment of inertia of the neutron star, P its period, $\dot{P}$ the time derivative of the period.

The response of the neutron star may be more intricate because a possible superfluid interior may not be coupled completely rigidly to the crust and the magnetic field. Thus differential rotation between various components on various time scales might occur, while the immediate response would involve only the moment of inertia of the crust (many aspects of these phenomena have been discussed in Pines et al., 1981, and many other papers by the same group [ref. see Pines et al., 1981)]. These modifications would, however, concern mainly noise-like period fluctuations. The long-term (long as compared to the period) quasi stationary time-changes of the period will be discussed by assuming a rigid body rotation of the neutron star.

In the model discussed above, the Kelvin-Helmholtz instability leads to a turbulent diffusion of disk matter onto the magnetic field lines – in the manner described in Paper I. Although the whole disk surface is unstable we want to consider here the mass flow out of the disk only in a thin ring around the corotation radius r_c. Such an assumption is of course a restriction of the general case and one would expect that the formulae for the gain and loss of angular momentum given below will have to be modified. But since in this general case the flow pattern will be extremely complicated it is not clear at present what the exact formulae will be. As a first attempt we therefore restrict our discussion here to the accretion originating from such a narrow ring. This can be a reasonable description, if the mass flow falls off sufficiently rapidly with increasing r and if the inner edge of the disk is close to r_c, such that only the region around r_c is important for the rotational state of the neutron star. For $r > r_c$ corotating matter experiences an effective outward acceleration $g_{\text{eff}} = (3GM/r_c^2)\,(r - r_c)$, and at a certain radius $r_{eq} \equiv r_c x_{eq}$ it leaves the magnetic field lines. The braking torque depends on this radius r_{eq}, and the angular momentum exchange is

$$\delta J_b = \dot{M}_{\text{out}}\,\Omega r_c^2 (x_{eq}^2 - 1)\,. \tag{4.2}$$

The acceleration of the star is due to infalling matter for $r < r_c$

$$\delta J_{\text{acc}} = \dot{M}_{\text{in}}\,\Omega r_c^2\,. \tag{4.3}$$

If we take $\dot{M}_{\text{in}} = \dot{M}_{\text{out}} = \dot{M}$, then the rate of angular momentum change can be written as

$$\delta J = \dot{M}\Omega r_c^2 (2 - x_{eq}^2)\,. \tag{4.4}$$

A complete balance – $\delta J = 0$ – can be achieved by setting $x_{eq} = 1.4$. In a detailed model (which we do not have yet) x_{eq} would be determined by the balance of the magnetic field energy density and the kinetic energy density of the outflowing matter. The present status of our model leaves $\dot{M}_{\text{out}}$ and x_{eq} essentially as free parameters.

We have shown in Paper I that subsonic massflow out of the disk of a typical magnitude $\dot{M} = 10^{17}$ g/s, in a thin ring around r_c does not lead to unreasonable requirements on the physics of this

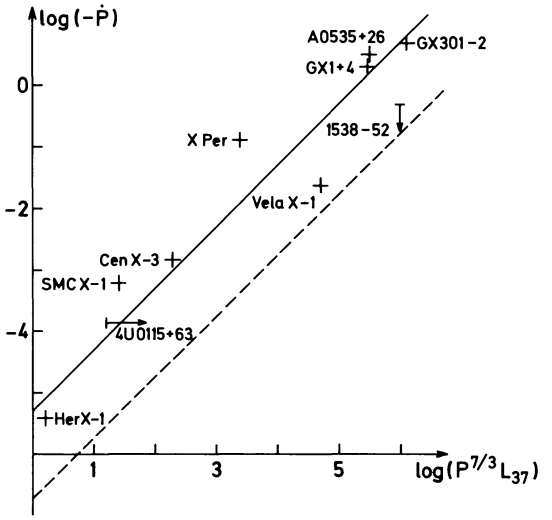

Fig. 5. A plot of $\dot{P}$ versus $\alpha P^{7/3}\dot{M}$ (with $\alpha=0.05$) compared to the observations. Vela X-1 is plotted in its spin-up phase (see Table 1). The dotted line corresponds to a white dwarf of $1\,M_\odot$

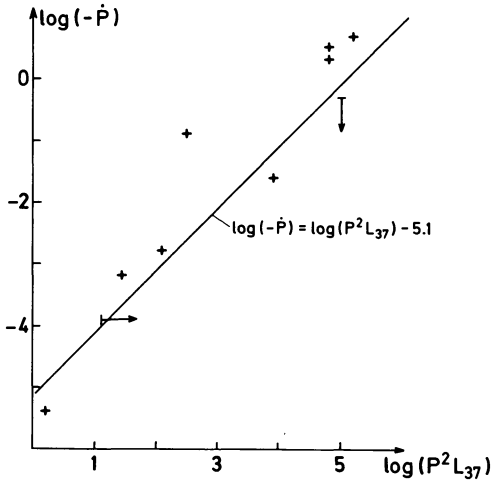

Fig. 6. Same as Fig. 5 with transfer of Keplerian angular momentum at the neutron star surface

turbulent diffusion process. If we set $\alpha=2-x_{eq}^2$, then the observations give spin-up time scales which are consistent with values of α around 0.05, if we take typical values for the neutron star of $M=1\,M_\odot$, $I=10^{45}$ gcm^2 assuming $\dot{M}=10\,L_x/c^2$. Such a low value of α indicates that the loss and the gain of angular momentum are well balanced in most sources.

In the model of Ghosh and Lamb (1979) the acceleration is due to the torque of the accreting matter, and the braking occurs through a magnetic torque acting in an extended transition zone outside of r_c. This transition zone, where field lines thread the disk, but do not control the motion, must reach very far out to achieve a close balance between acceleration and braking. Ghosh and Lamb (1979) take α as a function of the period P and the magnetic field B, and they obtain a good fit to the observations with $B\simeq 5\,10^{11}$ Gauss ($M=1.3\,M_\odot$) for all sources. There is a problem here, because Her X-1 has a measured value (Trümper et al., 1978)

Table 1

Source	L_x (2–11 keV) (erg s^{-1})	Period (s) $\dot{P}/P$ per year	Remarks
Her X−1	1E37	1.24 −3E−6	Spin-down episodes
4U0115+63	3E37	3.61 −3E−5	Transient
SMC X−1	6E38	0.71 −6E−4	
Cen X−3	4E37	4.84 −3E−4	Spin-down episodes
X Per	1.2E34	835 −2E−4	
Vela X−1	1.4E36	283 −2E−4	Since 1979 $\dot{P}/P=+3E-4$ (Oda and Tanaka, 1981)
4U1538−52	4E36	529 < −9.7E−4	
GX 1+4	4E37	121 −2E−2	
4U1728−24			
A0535+26	2E37	104 −2E−4	Recurring nova
GX301−2			Highly variable
4U1223−624	1E37	699 −1E−2	

of $B=5\,10^{12}$ Gauss. Ghosh and Lamb try to reconcile their model with this measurement by invoking a strong quadrupole component near the stellar surface – which represents the measured field – and a much weaker dipole component corresponding to their theoretical prediction.

In our opinion the fits to the data are at present only consistency checks on the models. No strong conclusions about the nature of the physical processes involved are possible. We have already pointed out that a good fit to the data can be obtained by setting $\delta J=\alpha\Omega r_c^2\dot{M}$ with $\alpha=0.05$. According to (4.1) this gives a relation

$$\dot{P}=\alpha P^{7/3}\dot{M}\frac{(GM)^{2/3}}{(2\pi)^{4/3}I}. \tag{4.5}$$

We have plotted the observational data points, and the theoretical relation of $\dot{P}$ vs. $P^{7/3}M$ in Fig. 5. Some numerical values are presented in Table 1 (cf. Börner, 1980; Bradt et al., 1979). We have assumed $M=M_\odot$, $I=10^{45}$ gcm^2 for all neutron stars. The luminosity L_x between 1 and 10 keV has been related to $\dot{M}$, via $L_x=0.1c^2\dot{M}$.

The data points representing the observations show a large scatter which is only partially due to the uncertainties of the observations. There is certainly also an intrinsic scatter in the parameters of the X-ray sources: The neutron stars may well have different values of M, I, B etc. These obvious uncertainties prohibit definite conclusions from the observations. White dwarfs can definitely be excluded as possible candidates, however. To demonstrate how unconvincing these fitting procedures are in distinguishing between different models, we have plotted the following very unrealistic relation (in Fig. 6): Assume that the

accretion disk reaches all the way to the neutron star, and transfers only its Keplerian angular momentum at the stellar radius:

$$\delta J = \dot{M}(GMR_*)^{1/2}, \tag{4.6}$$

i.e.

$$P = \frac{\dot{M}}{2\pi I}(GMR_*)^{1/2}P^2. \tag{4.7}$$

Then a curve is obtained which does fit the data not any worse than the other models (see Fig. 6).

Acknowledgements. We thank F. Meyer for helpful and clarifying discussions.

References

Aly, J.J.: 1980, *Astron. Astrophys.* **86**, 192
Anzer, U., Börner, G.: 1980, *Astron. Astrophys.* **83**, 133 (Paper I)
Börner, G.: 1980, *Physics Reports* **60**, 151
Bradt, W.V., Doxsey, R.E., Jernigan, J.G.: 1979, *Adv. in Space Expl.* **3**
Fejer, J.A.: 1964, *Phys. of Fluids* **7**, 499
Ghosh, P., Lamb, F.K.: 1979a, *Astrophys. J.* **232**, 259
Ghosh, P., Lamb, F.K.: 1979b, *Astrophys. J.* **234**, 296
Ghosh, P., Lamb, F.K., Pethick, C.: 1977, *Astrophys. J.* **217**, 578
Kundt, W., Robnik, M.: 1980, *Astron. Astrophys.* **91**, 305
Oda, M., Tanaka, Y.: 1981, ISAS Research Note
Pines, D., Shaham, J., Alpas, M.A., Anderson, P.W.: 1981, Urbana preprint
Riffert, H.: 1980, *Astrophys. Space Sci.* **71**, 195
Trümper, J., Pietsch, W., Reppin, C., Voges, W., Staubert, R., Kendziorra, E.: 1978, *Astrophys. J.* **219**, L 105